

# An Empirical Approach for Predicting Retention Characteristics in Supercritical Fluid Chromatography

Somenath Mitra\*, Feinan Shi, and Jun Du

Department of Chemical Engineering, Chemistry, and Environmental Science, New Jersey Institute of Technology, Newark, New Jersey

## Abstract

The retention process in supercritical fluid chromatography depends on the solute volatility as well as the strength of the mobile phase. When the capacity factor is plotted as a function of temperature at constant pressure, the curve passes through a maximum point. At higher temperatures, the capacity factor decreases as the temperature increases, and at lower temperatures the opposite is observed. This makes prediction of the capacity factor in supercritical fluid chromatography complicated. Rigorous thermodynamic equations to predict retention characteristics result in complex equations. A simple empirical approach for prediction of the capacity factor as a function of mobile phase density and column temperature is presented.

## Introduction

Supercritical fluid chromatography (SFC) occupies the middle ground between gas chromatography (GC) and liquid chromatography (LC). Retention in gas chromatography depends on the solute volatility and the solute-stationary phase interactions. Because both these factors are temperature dependent, retention is usually controlled by changing the column temperature. In LC, however, it is the strength of the mobile phase rather than the temperature which controls retention. Retention in chromatography is usually measured as the capacity factor ( $k'$ ):

$$k' = \frac{t_R - t_0}{t_0} \quad \text{Eq 1}$$

where  $t_R$  is the retention time and  $t_0$  is the time required by an unretained substance to elute from the column. In GC,  $k'$  decreases as the column temperature is increased. In LC,  $k'$  decreases with an increase in the strength of the mobile phase. In SFC, the solute volatility and the strength of mobile phase play important roles. The solute volatility depends on the

column temperature, and the strength of the supercritical mobile phase depends on its state of compression, or density. Typical variation of  $k'$  as a function of temperature and pressure is shown in Figure 1. At higher temperatures, SFC behaves like GC, that is,  $k'$  decreases as temperature increases when pressure is held constant. This GC-type behavior is attributed to solute volatility, which increases with temperature. However, at lower temperatures, the opposite is observed: the capacity factor increases when temperature is increased and pressure remains constant. As the temperature increases, the density of the supercritical fluid decreases, reducing its solvent strength. In this region, it is the strength of the mobile phase rather than the volatility which plays an important role. SFC exhibits LC-type behavior where  $k'$  decreases with increased solvent strength. This phenomenon is used in SFC for reverse temperature programming (1,2), which serves the same purpose as gradient elution in LC. As a result of GC- and LC-type mechanisms, a maximum is observed when the capacity factor is plotted as a function of temperature at constant pressure. This phenomenon has been reported for a variety of mobile phase-analyte systems (3-7).

Several papers in the literature describe attempts to model the retention process in SFC, that is, to predict the capacity factor as a function of temperature, pressure, or density. GC- and LC-type behavior are difficult to model, and no comprehensive predictive model is available at this point. Rigorous thermodynamic models using equations of state have been proposed (8,9). However, even a simple two-constant equation of state results in a complex algebraic equation that may not have unique solutions and may have to be solved numerically. These models also require the knowledge of certain thermodynamic parameters that are not readily available in the literature and need to be determined experimentally. Several researchers have reported a linear relationship between the logarithm of the capacity factor and density at constant temperature (3). At higher densities, some investigators have reported (4,10) deviation from the linear relationship and suggest a logarithmic relationship:

$$\log k' = a + b \log p \quad \text{Eq 2}$$

\* Author to whom correspondence should be addressed.

where  $a$  and  $b$  are temperature-dependent constants. Luffer and co-workers (11) expanded Equation 2 to develop an empirical equation for the capacity factor of polycyclic aromatic hydrocarbons. The logarithm of the capacity factor was also shown to correlate with density (at constant temperature) in a quadratic form (12,13).

Chester and Innis (3) tried to correlate retention in SFC and GC. They computed the enthalpy of interaction between the solute and the stationary phase from the slope of a van't Hoff plot of  $\ln k'$  versus the inverse of temperature ( $1/T$ ). In SFC, this plot is a straight line at the higher temperatures where GC-type behavior is observed. At low temperatures (and higher densities), when the solvating effect becomes the dominant factor (LC-type behavior), deviation from linearity is observed. The difference between the extrapolated straight line and  $k'$  at any given temperature was attributed to solute–mobile phase interaction at that point. Berger (4) extended this approach to a model of the following form:

$$\log k'_{\text{SFC}} = -\frac{\Delta H_{\text{s-sp}}}{RT} + \frac{d(\Delta H_{\text{s-mp}} + \Delta H_{\text{mp-sp}})}{RT} \quad \text{Eq 3}$$

The first term in this equation accounts for the solute–stationary phase interaction, which was assumed to be same for GC and SFC and was computed using van't Hoff plots.  $\Delta H_{\text{s-mp}}$  and  $\Delta H_{\text{mp-sp}}$  denote enthalpies of solute–mobile phase and mobile phase–stationary phase interactions and account for the LC-type behavior. The enthalpy of interaction between the mobile phase and the solute depends on density. Thus, application of this model requires the knowledge of enthalpy as a function of density. Martire (13) proposed a general equation that derives the capacity factor:

$$\ln k' = \ln k'_0 + f(T_R, \rho_R) \quad \text{Eq 4}$$

where  $\ln k'_0$  is the stationary phase contribution, corresponding to the ideal gas–liquid chromatography. The mobile phase contribution is accounted for by the second term. The model was expanded for retention of  $n$ -alkanes in the  $\text{CO}_2$  mobile phase:

$$\ln \left( \frac{k'}{k'_0} \right) = \left( \frac{r_a}{r_b} \right) \left[ 1.148(\rho_R) - 0.2784 \left( \frac{\rho_R}{T_R} \right) + 0.500 \left( \frac{\rho_R^2}{T_R} \right) \right]$$

$$\text{Eq 5}$$

$r_a$  and  $r_b$  are estimated from the ratio of the respective van der Waals volumes.

Sakaki and co-workers (14) applied the retention mechanisms of reversed-phase liquid chromatography to SFC. The free energy change ( $\Delta G^\circ$ ) of the solute transfer was expressed as:

$$\Delta G^\circ = \Delta G_{\text{vdw}}^\circ - \Delta G_c^\circ - \Delta G_{\text{int}}^\circ - RT \ln \left[ \frac{RT}{P_0 V} \right] \quad \text{Eq 6}$$

where  $\Delta G_{\text{vdw}}^\circ$  is the free energy change contribution to the interaction between the solutes and ligand;  $\Delta G_c^\circ$  is the free energy of solute transfer between the stationary phase to mobile phase based on the creation of a solute-sized cavity in mobile phase; and  $\Delta G_{\text{int}}^\circ$  accounts for the interaction between the solute with solvent.  $P_0$  is the pressure;  $V$  is the molar volume of the solvent; and  $\beta$  is the ratio of the mobile phase to the stationary phase volume.  $\Delta G_c^\circ$  is considered negligible for SFC, and retention was described as follows:

$$\ln k' = -\ln \beta - \frac{\Delta G_{\text{vdw}}^\circ}{RT} + \frac{\Delta G_{\text{int}}^\circ}{RT} + \ln \left[ \frac{RT}{P_0 V} \right] \quad \text{Eq 7}$$

Some of the previously mentioned models have described specific experimental data adequately. Theoretical models based on thermodynamic principles are complex and require the knowledge of certain parameters and constants that are not easily available. As observed in the previous discussion, several empirical relationships have described the variation of  $k'$  with density at constant temperature, but no comprehensive model that predicts  $k'$  as a function of density and temperature is available.

The objective of this investigation was to develop a simple model that can predict retention in SFC as a function of temperature and density. In other words, from the knowledge of  $k'$  at a few points in temperature and density,  $k'$  can be predicted at all other operating conditions. The models developed here are compared with models available from the literature.

### Description of data

Two sets of data from the literature were used for developing empirical correlation:  $k'$  for hexadecane in  $\text{CO}_2$  (3) and  $k'$  for fluoranthene in  $\text{CO}_2$  (4). The  $\text{CO}_2$ –fluoranthene system consisted of six capacity factor isobars between 90 and 140 atm measured in the range of 35–220°C with a methyl silicone capillary column. The  $\text{CO}_2$ –hexadecane data consisted of four capacity factor isobars between 81 and 115.7 atm that were measured in the range of 31–70°C with a BP-10 capillary column. In each data set, the GC-type and the LC-type behavior could be seen, and the capacity factor maxima

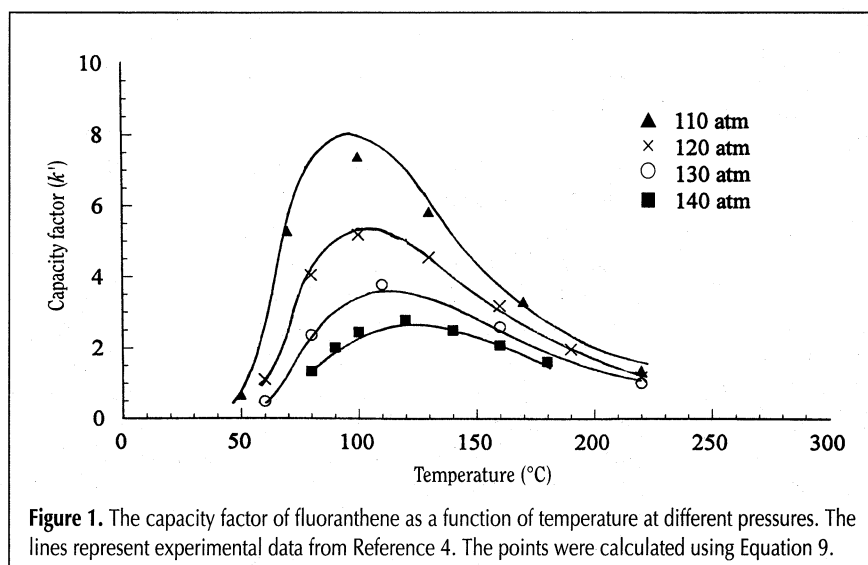


Figure 1. The capacity factor of fluoranthene as a function of temperature at different pressures. The lines represent experimental data from Reference 4. The points were calculated using Equation 9.

was present. Additional sets of data consisting of the capacity factor measurements of different organic molecules in ethane, N<sub>2</sub>O, pentane, and CO<sub>2</sub> (1,3–5,15) were examined to see if they showed similar behavior. Data from both packed and capillary columns were analyzed. A list of the data sets studied is presented in Tables I and II.

### Data analysis

Retention in SFC is sensitive to density (16), so accurate computation of density at different temperatures and pressures was important in this analysis. Experimental values of the density of CO<sub>2</sub> at different temperatures and pressures were published by Vuklovich and Altunin (17), but these are incomplete at some temperature ranges, especially near the critical region. Therefore, the density of CO<sub>2</sub> was computed from density tables supplied by the Lee Scientific Division of Dionex Corp. (Salt Lake City, UT). The Lee Scientific density tables are generated using a two-constant equation of state. There was good agreement between the Lee Scientific densities and the experimental values of Vuklovich and Altunin (17). The densities of N<sub>2</sub>O, pentane, and ethane were also calculated using the Lee Scientific tables. Multiple regression was used to find a relationship between the capacity factor, temperature, and density using the Statgraphics statistical analysis package (STSC, Inc.; Rockville, MD).

## Results and Discussion

Of temperature, pressure, and density, only two parameters may be considered independent variables. Density of a supercritical fluid is normally computed as a function of temperature and pressure using an equation of state. At any given tempera-

ture, density increases with an increase in pressure; and at any given pressure, density decreases with an increase in temperature.

The variations of the capacity factor of fluoranthene with temperature and pressure are presented in Figure 1. As mentioned previously, the capacity factor is known to correlate more closely with density than with pressure. Therefore, temperature and density were chosen as the independent variables. To see what combination of temperature and density resulted in the same  $k'$  values, density and temperature were plotted against one another at constant capacity factor (see Figure 1). The results for retention of fluoranthene in CO<sub>2</sub> are shown in Figure 2. At a certain  $k'$  value, the plot of temperature versus density results in a straight line. In other words, when the column temperature was increased, the density had to be decreased to keep the capacity factor constant. A series of parallel lines was obtained that represented different values of  $\log k'$ . A similar relationship between density and temperature at a constant capacity factor was also observed for retention of hexadecane in CO<sub>2</sub>. These data are not presented here for the sake of brevity.

Because density and temperature were linearly correlated at a constant  $k'$ , it may be inferred that

$$f(k') = a' + b'\rho + c'T \quad \text{Eq 8}$$

where  $f(k')$  is some function of  $k'$ ;  $T$  and  $\rho$  are temperature and density, respectively; and  $a'$ ,  $b'$ , and  $c'$  are constants. The relationship between the capacity factor, temperature, and density was obtained by multiple regression. The logarithm of the capacity factor correlated with reduced density (density/critical density) and reduced temperature (temperature/critical temperature in degrees Kelvin) as:

$$\ln k' = a + b\rho_R + c T_R \quad \text{Eq 9}$$

**Table I. Coefficient of Temperature–Density Model (Equation 9):  $\ln k' = a + b\rho_R + c T_R$**

	<i>a</i>	SE* of <i>a</i>	<i>b</i>	SE of <i>b</i>	<i>c</i>	SE of <i>c</i>	<i>r</i> <sup>2</sup>	Model SE	Column	Reference
<i>CO<sub>2</sub> as mobile phase</i>										
Dodecane (C <sub>14</sub> ) in CO <sub>2</sub>	9.46	0.44	-4.61	0.22	-6.86	0.29	0.98	0.08	Capillary	3
Tetradecane (C <sub>14</sub> ) in CO <sub>2</sub>	10.7	0.99	-4.54	0.43	-7.21	0.69	0.89	0.20	Capillary	3
Hexadecane (C <sub>16</sub> ) in CO <sub>2</sub>	15.8	0.41	-6.71	0.18	-10.1	0.28	0.98	0.12	Capillary	3
Nonanoic acid	12.2	0.93	-3.84	0.40	-8.38	0.61	0.96	0.10	Capillary	3
Benzo[ <i>e</i> ]pyrene	11.4	0.66	-4.34	0.25	-5.56	0.37	0.98	0.04	Capillary	3
Perylene	13.8	0.33	-5.45	0.16	-6.73	0.18	0.99	0.02	Capillary	4
Fluoranthene	13.4	0.45	-5.82	0.20	-7.12	0.27	0.97	0.11	Capillary	4
Chrysene	10.5	0.34	-4.01	0.14	-5.44	0.19	0.99	0.02	Capillary	4
Chrysene	14.6	0.65	-3.45	0.18	-6.53	0.37	0.92	0.15	Packed	15
2-Nitrotoluene	12.1	0.34	-6.68	0.21	-7.99	0.24	0.99	0.11	Capillary	5
3-Nitrotoluene	12.6	0.26	-7.36	0.16	-8.09	0.19	1.00	0.24	Capillary	5
4-Nitrotoluene	12.6	0.25	-6.93	0.17	-8.05	0.18	0.99	0.09	Capillary	5
<i>C<sub>2</sub>H<sub>6</sub> as mobile phase</i>										
Chrysene	22.0	1.46	-7.75	0.68	-9.55	0.70	0.90	0.21	Packed	15
<i>N<sub>2</sub>O as mobile phase</i>										
Chrysene	16.6	0.65	-4.20	0.15	-7.85	0.39	0.99	0.21	Packed	15
<i>Pentane as mobile phase</i>										
Biphenyl	11.5	3.22	-1.91	0.19	-8.13	3.02	0.94	0.19	Packed	1

\* Standard error.

where  $a$ ,  $b$ , and  $c$  are constants, and  $\rho_R$  and  $T_R$  represent mobile phase reduced density and reduced temperature, respectively.

Several data sets representing different analyte–mobile phase combinations were correlated using Equation 9, and the results are presented in Table I. It can be seen in Table I that the capacity factor of both polar and nonpolar solutes may be predicted using Equation 9. The data from packed and capillary columns appear to fit this model. The data sets studied here represent a reasonably wide range of capacity factors, temperatures, and densities (or pressures) that one may expect to encounter in SFC.

The significance level, expressed as the probability that the values of a certain constant ( $a$ ,  $b$ ,  $c$ ) were 0, was less than 5% for all the analyte–mobile phase systems. The distribution of residuals was also random, indicating that there were no systematic deviations in the model. The square of the multiple regression coefficient,  $r^2$ , is a measure of variance explained by the model. For all the systems studied here,  $r^2$  was found to be between 0.89 and 0.99. The high  $r^2$  values obtained for so many diverse systems indicate that Equation 9 describes the relationship between the capacity factor, temperature, and density adequately. As a result, the model values in Figure 1 using Equation 9 are in agreement with the experimental results. Equation 9 also appears to predict the position of the maxima in Figure 1.

The term  $b \rho_R$  accounts for the solvating effect of the mobile phase, and  $c T_R$  accounts for the volatility effect. The magnitude of constants  $b$  and  $c$  determines the relative dependence of the capacity factor on temperature and density. These values depend on the analyte, the mobile phase, the stationary phase, and the type of column (capillary or packed). These constants are independent of temperature, pressure, and density. The

ratio of  $c$  to  $b$  is the slope of the constant capacity factor line in Figure 2.

In 1991, empirical equations for predicting equilibrium solubility of solutes in supercritical fluids as a function of temperature and density were published (18). When density and temperature were plotted against one another at constant solubility, parallel lines similar to Figure 2 were obtained (19). This showed that when temperature was increased, density had to be decreased to keep the solubility constant. It was found that the logarithm of solubility correlated with density and temperature in a manner similar to Equation 9. Unlike  $k'$ , solubility increases with temperature and density, and the coefficients  $b$  and  $c$  have positive values. This demonstrates that retention of a certain analyte in SFC is closely related to its solubility in the mobile phase. This is in agreement with the published hypothesis that the capacity factor is inversely proportional to solubility (19,20).

Equation 9 is applicable only in the temperature–pressure–density region studied, although the data used in this study included a wide range of  $k'$  values (0.2–50). At higher densities, stronger intermolecular interactions may cause deviation from Equation 9. As discussed previously, at high mobile phase densities where  $k'$  is rather small, the relationship between  $k'$  and density at constant temperature tends to be nonlinear.

Bartle and co-workers (20) reported that  $k'$  and solubility are related as follows:

$$k' = \frac{C}{S} \quad \text{Eq 10}$$

where  $S$  is solubility and  $C$  is a temperature dependent constant.  $C$  varies as a function of temperature as (21):

**Table II. Coefficient of Temperature–Density Model (Equation 14):  $\ln k' = a + b \ln \rho_R + c T_R$**

	$a$	SE* of $a$	$b$	SE of $b$	$c$	SE of $c$	$r^2$	Model SE	Column	Reference
<i>CO<sub>2</sub> as mobile phase</i>										
Dodecane (C <sub>14</sub> ) in CO <sub>2</sub>	6.31	0.47	-2.37	0.17	-7.68	0.48	0.95	0.12	Capillary	3
Tetradecane (C <sub>14</sub> ) in CO <sub>2</sub>	8.24	0.67	-2.69	0.21	-8.84	0.67	0.92	0.17	Capillary	3
Hexadecane (C <sub>16</sub> ) in CO <sub>2</sub>	11.5	0.46	-3.73	0.15	-11.6	0.46	0.96	0.17	Capillary	3
Nonanoic acid	10.9	1.03	-2.71	0.36	-10.6	1.06	0.94	0.13	Capillary	3
Benzo[e]pyrene	11.2	0.51	-4.59	0.21	-9.13	0.45	0.99	0.03	Capillary	3
Perylene	12.5	0.55	-5.09	0.27	-10.2	0.51	0.99	0.03	Capillary	4
Fluoranthene	10.6	0.69	-4.38	0.28	-9.61	0.65	0.91	0.21	Capillary	4
Chrysene	10.1	0.35	-4.05	0.15	-8.53	0.31	0.99	0.02	Capillary	4
Chrysene	12.0	0.99	-3.42	0.34	-7.31	0.78	0.76	0.26	Packed	15
2-Nitrotoluene	6.85	0.74	-2.75	0.26	-8.12	0.70	0.93	0.30	Capillary	5
3-Nitrotoluene	6.84	0.54	-3.08	0.19	-8.25	0.51	0.96	0.24	Capillary	5
4-Nitrotoluene	7.02	0.55	-2.81	0.20	-7.98	0.51	0.95	0.26	Capillary	5
<i>C<sub>2</sub>H<sub>6</sub> as mobile phase</i>										
Chrysene	12.8	1.17	-4.52	0.69	-8.17	1.01	0.76	0.32	Packed	15
<i>N<sub>2</sub>O as mobile phase</i>										
Chrysene	14.1	1.60	-4.78	0.48	-9.51	1.26	0.89	0.28	Packed	15
<i>Pentane as mobile phase</i>										
Biphenyl	8.45	0.52	-1.30	0.02	-7.18	0.50	0.99	0.03	Packed	1

\* Standard error.

$$C = Ae(B/T) \quad \text{Eq 11}$$

Chrastil and co-workers (22) correlated solubility as a function of density ( $\rho$ ):

$$\ln S = n \ln \rho - \frac{\Delta H_m^\circ}{RT} + C' \quad \text{Eq 12}$$

where  $C'$  is constant, and  $\Delta H_m^\circ$  is the enthalpy of solvation and vaporization. This was assuming that at equilibrium, one molecule of a solute associated with  $n$  molecules of solvate complex. Replacing the solubility by Equation 12, one can predict the equation:

$$\ln k' = -n \ln \rho + (B - \Delta H_m^\circ/R)/T + \ln A + C \quad \text{Eq 13}$$

which can be rearranged as follows:

$$\ln k' = a + b \ln \rho_R + c T_R \quad \text{Eq 14}$$

where  $a$ ,  $b$ , and  $c$  are constants. The results from this correlation are presented in Table II. The same analyte–mobile phase systems were studied. The values of  $r^2$  were found to be between 0.76 and 0.99, showing relatively good correlation between  $k'$ , density, and temperature. The significance levels for all the constants  $a$ ,  $b$ , and  $c$  were also below the 5% level for all analyte–mobile phase systems.

For a certain analyte–mobile phase system, one of the previously mentioned equations may be more appropriate than the other. Based on data presented in Tables I and II, there is no clear indication as to which equation is a better model overall. Further research is necessary in this area to make a determination. Judging by literature reports (4,10), Equation 14 may be expected to provide a better fit for measurements at low  $k'$ . However, chromatography is seldom performed at very low or very high capacity factors. Consequently, from a practical point of view, Equation 9 may be expected to work well for most systems.

It would be more convenient to have a model in terms of pressure rather than density because pressure is an actual process parameter, whereas density is not. Density may be

substituted in Equations 9 and 14 as a function of temperature and pressure. However, even simple equations of state such as the Peng–Robinson or Redlich–Kwong result in quadratic equations with multiple roots, making direct substitution difficult. Therefore, it is easier to simply compute the operating pressure from density and temperature. The advantage of models such as Equations 9 and 14 is that from a minimum of three experimental measurements the constants  $a$ ,  $b$ , and  $c$  can be computed, and the capacity factor can be predicted in a wide range of temperatures and densities (or pressures). Consequently, these equations can be useful in optimizing chromatographic conditions. The simplicity of these equations is an added advantage because they can be readily employed in developing other relationships in SFC.

Two candidate empirical models based on the work by Martire (13) and Sakaki and co-workers (14) were also tried. The model from Martire presented in Equation 5 may be rearranged as follows:

$$\ln(k') = a + b(\rho_R) - c \left( \frac{\rho_R}{T_R} \right) + d \left( \frac{\rho_R^2}{T_R} \right) \quad \text{Eq 15}$$

where  $a$ ,  $b$ ,  $c$ , and  $d$  are assumed to be constants independent of  $T_R$  and  $\rho_R$ .

Another model can be developed by modifying the model published by Sakaki and co-workers (14). Because density is equal to mass ( $M$ ) divided by volume ( $V$ ), Equation 7 can be reduced to the following:

$$\ln k' = -\ln \beta - \frac{\Delta G_{\text{vdw}}^\circ}{RT} + \frac{\Delta G_{\text{int}}^\circ}{RT} + \ln \left[ \frac{RT \rho}{P_0 M} \right] \quad \text{Eq 16}$$

Assuming  $\Delta G_{\text{vdw}}^\circ$ ,  $\Delta G_{\text{int}}^\circ$ , and  $M$  to be constants, Equation 16 may be rearranged as a function of reduced temperature and reduced density:

$$\ln k' = a + b \ln \rho_R + \frac{c}{T_R} + d \ln T_R \quad \text{Eq. 17}$$

where  $a$ ,  $b$ ,  $c$ , and  $d$  are constants independent of temperature and density.

Equations 15 and 17 have four constants and require more data points for model validation. Five data sets of fluoranthene in  $\text{CO}_2$ ; chrysene in  $\text{CO}_2$ ,  $\text{N}_2\text{O}$ , and  $\text{C}_2\text{H}_6$ ; and hexadecane in  $\text{CO}_2$  were used compare the models because each of them contained a relatively large number of measurement at multiple pressures. The result is presented in Table III. It is seen that Equations 9 and 14 provide better fits than Equations 15 and 17. The standard errors were lower. The model based on Sakaki's equation did not hold well for the hexadecane– $\text{CO}_2$  system. The standard errors of constants were high, and the significance levels for two of the constants were as high as 0.21. Consequently, this model was rejected. Martire's model appears to fit all the data sets, but the standard errors for the hexadecane– $\text{CO}_2$  and chrysene– $\text{CO}_2$  systems were higher than those obtained by

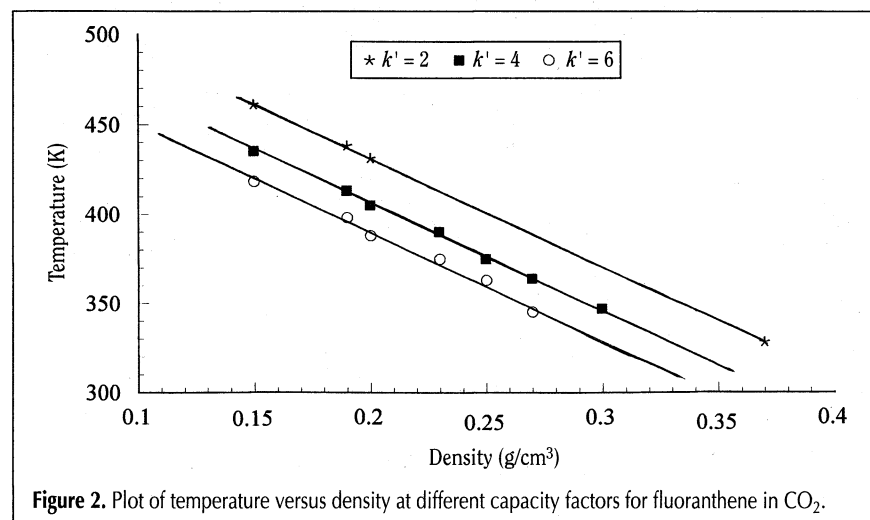


Figure 2. Plot of temperature versus density at different capacity factors for fluoranthene in  $\text{CO}_2$ .

Table III. Comparison of Various Models

	a	SE of a	b	SE of b	c	SE of c	d	SE	r <sup>2</sup>	Model SE	Reference
<i>Fluoranthene in CO<sub>2</sub></i>											
$\ln k' = a + b\rho_R + cT_R$	13.4	0.45	-5.82	0.20	-7.12	0.27			0.97	0.11	4, Capillary
$\ln k' = a + b \ln \rho_R + cT_R$	10.6	0.69	-4.38	0.28	-9.61	0.65			0.91	0.21	
$\ln k' = a + b \ln \rho_R + c/T_R + d \ln T_R$	31.4	7.81	-30.9	7.81	-4.02	0.33	-35.2	5.54	0.92	0.20	
$\ln k' = a + b\rho_R + c\rho_R/T_R + d\rho_R^2/T_R$	2.14	0.39	-23.3	2.79	31.76	2.88	-8.73	0.74	0.91	0.21	
<i>Chrysene in CO<sub>2</sub></i>											
$\ln k' = a + b\rho_R + cT_R$	14.6	0.65	-3.45	0.18	-6.53	0.37			0.92	0.15	15, Packed
$\ln k' = a + b \ln \rho_R + cT_R$	12.0	0.99	-3.42	0.34	-7.31	0.78			0.76	0.26	
$\ln k' = a + b \ln \rho_R + c/T_R + d \ln T_R$	295	16.9	-2.92	0.16	-46.0	3.20	-43.0	2.41	0.95	0.12	
$\ln k' = a + b\rho_R + c\rho_R/T_R + d\rho_R^2/T_R$	3.26	0.37	-9.87	1.76	15.7	2.33	-3.62	0.52	0.67	0.31	
<i>Chrysene in N<sub>2</sub>O</i>											
$\ln k' = a + b\rho_R + cT_R$	16.6	0.65	-4.20	0.15	-7.85	0.39			0.99	0.10	15, Packed
$\ln k' = a + b \ln \rho_R + cT_R$	14.1	1.60	-4.78	0.48	-9.51	1.26			0.89	0.28	
$\ln k' = a + b \ln \rho_R + c/T_R + d \ln T_R$	54.1	10.5	-4.28	0.40	-50.6	10.8	-50.1	8.15	0.94	0.21	
$\ln k' = a + b\rho_R + c\rho_R/T_R + d\rho_R^2/T_R$	3.99	0.32	-13.2	1.35	17.9	1.65	-3.22	0.33	0.96	0.17	
<i>Chrysene in C<sub>2</sub>H<sub>6</sub></i>											
$\ln k' = a + b\rho_R + cT_R$	22.0	1.46	-7.75	0.68	-9.55	0.70			0.90	0.21	15, Packed
$\ln k' = a + b \ln \rho_R + cT_R$	12.8	1.17	-4.52	0.69	-8.17	1.01			0.76	0.32	
$\ln k' = a + b \ln \rho_R + c/T_R + d \ln T_R$	46.0	7.03	-4.54	0.53	-42.3	7.21	-42.5	5.64	0.85	0.25	
$\ln k' = a + b\rho_R + c\rho_R/T_R + d\rho_R^2/T_R$	4.85	0.39	27.2	1.90	-17.7	1.13	-232	20.4	0.92	0.18	
<i>Hexadecane in CO<sub>2</sub></i>											
$\ln k' = a + b\rho_R + cT_R$	15.8	0.41	-6.71	0.18	-10.1	0.28			0.98	0.12	4, Capillary
$\ln k' = a + b \ln \rho_R + cT_R$	11.5	0.46	-3.73	0.15	-11.6	0.46			0.96	0.12	
$\ln k' = a + b \ln \rho_R + c/T_R + d \ln T_R$	13.5 <sup>†</sup>	10.5	-3.74	0.15	-13.6 <sup>†</sup>	10.7	-25.4	8.77	0.86	0.17	
$\ln k' = a + b\rho_R + c\rho_R/T_R + d\rho_R^2/T_R$	1.93	0.43	-30.5	2.70	36.3	2.27	-7.88	1.43	0.92	0.24	

\* Standard error

† Significance level over 0.05

Equations 9 and 14. Considering all these factors, including the additional constant in Martire's model, it was determined that Equations 9 and 14 are the most useful empirical models for predicting the capacity factor.

## Conclusion

Empirical equations for predicting the capacity factor as a function of reduced temperature and reduced density are presented. Several data sets representing different types of analytes, stationary phases, and mobile phases were studied. The equations developed here appear to model all the systems accurately.

## References

1. M. Novotny, W. Bertsch, and A. Zlatkis. *J. Chromatogr.* **61**: 17 (1971).
2. J.E. Conway, J.A. Graham, and L.B. Rogers. *J. Chromatogr. Sci.* **16**: 102-110 (1978).
3. T.L. Chester and D. Innis. *J. High Res. Chromatogr. Chromatogr. Comm.* **8**: 561 (1985).
4. T.A. Berger. *J. Chromatogr.* **478**: 311 (1989).
5. A. Munder, S.N. Chesler, and S.A. Wise. *J. Chromatogr.* **521**: 63 (1990).
6. F.P. Schmitz, D. Leyendecker, and E. Klesper. *Ber. Bunsenges. Phys. Chem.* **88**: 912 (1984).
7. D. Leyendecker, F.P. Schmitz, and E. Klesper. *J. Chromatogr.* **315**: 19 (1984).
8. J.P. Shoenmakers. *J. Chromatogr.* **315**: 1 (1984).
9. R.C. Yonkers, R.C. Wright, S.L. Fry, and R.D. Smith. In *Supercritical Fluids: Chemical and Engineering Principles and Applications*. ACS Symposium Series, No. 329, American Chemical Society, Washington, DC, 1987.
10. C.R. Yonker and R.D. Smith. *J. Phys. Chem.* **92**: 1664 (1988).
11. D.R. Luffer, W. Ecknig, and M. Novotny. *J. Chromatogr.* **505**: 79 (1990).
12. X. Zhang, D.E. Martire, and R.G. Christensen. *J. Chromatogr.* **603**: 193- (1992).
13. D.E. Martire. *J. Liq. Chromatogr.* **10**: 1569-88 (1987).
14. K. Sakaki, T. Shinbo, and M. Kawamura. *J. Chromatogr. Sci.* **32**: 172-78 (1994).
15. D. Leyendecker, D. Leyendecker, F.P. Schmitz, and E. Klesper. *J. Liq. Chromatogr.* **10**: 1917 (1987).
16. R.M. Smith. *Supercritical Fluid Chromatography*. Royal Society of Chemistry, London, U.K., 1988.

17. M.P. Vuklovich and V.V. Altunin, *Thermophysical Properties of CO<sub>2</sub>*. Collet Publishers Ltd., London, U.K., 1968.
18. S. Mitra and N.K. Wilson. An empirical method to predict solubility in supercritical fluids. *J. Chromatogr. Sci.* **29**: 305–309 (1991).
19. K.D. Bartle, A.A. Clifford, S.A. Jafar, J.P. Kithinji, and G.F. Shiltone. *J. Chromatogr.* **517**: 459 (1990).
20. K.D. Bartle, A.A. Clifford, and S.A. Jafar. *J. Chem. Soc. Faraday Trans.* **86**: 855 (1990).
21. M.L. Lee and K.E. Markdes. *Analytical Supercritical Fluid Chromatography and Extraction*. Chromatography Conference, Inc., Provo, UT, 1990. p 30.
22. J. Chrastil. Solubility of solids and liquids in supercritical gases. *J. Phys. Chem.* **86**: 3016–3021 (1981).

Manuscript accepted August 25, 1995.